Distribution of Choroidal Thickness and Choroidal Vessel Dilation in Healthy Japanese Individuals: The Nagahama Study

AUTHOR(S):

Mori, Yuki; Miyake, Masahiro; Hosoda, Yoshikatsu; Uji, Akihito; Nakano, Eri; Takahashi, Ayako; Muraoka, Yuki; ... Yamashiro, Kenji; Matsuda, Fumihiko; Tsujikawa, Akitaka

CITATION:

Mori, Yuki ...[et al]. Distribution of Choroidal Thickness and Choroidal Vessel Dilation in Healthy Japanese Individuals: The Nagahama Study. Ophthalmology Science 2021, 1(2): 100033.

ISSUE DATE:

2021-06

URL:

http://hdl.handle.net/2433/276764

AMERICAN ACADEMY OF OPHTHALMOLOGY®

Distribution of Choroidal Thickness and Choroidal Vessel Dilation in Healthy Japanese Individuals

The Nagahama Study

*Yuki Mori, MD,[1,2] Masahiro Miyake, MD, PhD,[1,2] Yoshikatsu Hosoda, MD, PhD,[3] Akihito Uji, MD, PhD,[1] Eri Nakano, MD,[1] Ayako Takahashi, MD, PhD,[1] Yuki Muraoka, MD, PhD,[1] Manabu Miyata, MD, PhD,[1] Hiroshi Tamura, MD, PhD,[1,4] Sotaro Ooto, MD, PhD,[1] Yasuharu Tabara, PhD,[2,5] Kenji Yamashiro, MD, PhD,[6] Fumihiko Matsuda, PhD,[2] Akitaka Tsujikawa, MD, PhD,[1] for the Nagahama Study Group**

Purpose: To report fundamental epidemiologic data for choroidal parameters such as choroidal thickness and index of choroidal vascularity in Japanese individuals and to evaluate their correlations with age, sex, systemic parameters, and other ocular parameters.

Design: Population-based cohort study.

Participants: A total of 9850 individuals participated in the first follow-up of the Nagahama Prospective Cohort for Comprehensive Human Bioscience (the Nagahama Study) conducted between 2013 and 2016.

Methods: All participants underwent standardized ophthalmic examinations, including OCT with enhanced depth imaging (EDI; RS-3000 Advance; Nidek). We manually segmented the choroidoscleral interface to measure subfoveal choroidal thickness (SFCT) and calculated the normalized choroidal intensity obtained with EDI (NCI_{EDI}) and choroidal vascularity index (CVI). These are indices of choroidal brightness in OCT and reportedly represent the dilation of choroidal vessels. After summarizing the age-sex stratified distributions of SFCT, NCI_{EDI}, and CVI, their associations with age, sex, axial length (AL), and spherical equivalent (SE) were evaluated using linear regression analysis with adjustments for possible confounders.

Main Outcome Measures: Distribution of SFCT, NCI_{EDI}, and CVI in the healthy Japanese population and their characteristics.

Results: Age-sex standardized SFCT, NCI_{EDI}, and CVI were 291.2 μm, 0.653, and 66.88%, respectively. In both men and women, SFCT was associated negatively with age ($P < 0.001$) and NCI_{EDI} was associated positively with age ($P < 0.001$). Although both SFCT and NCI_{EDI} did not differ significantly between men and women overall ($P = 0.87$ and $P = 0.21$, respectively), among younger participants (35−50 years of age), men showed significantly greater SFCT than women ($P < 0.001$). Only in men was CVI associated positively with age ($P < 0.001$). In the multivariable analysis, SFCT was associated significantly with age, sex, AL, SE, and the interaction term of age and sex ($P < 0.001$). Independent of SFCT, NCI_{EDI} and CVI were associated significantly with age ($P < 0.001$).

Conclusions: We report normative Japanese SFCT, NCI_{EDI}, and CVI data using a large general Japanese cohort. The association analysis of SFCT with NCI_{EDI} and CVI suggested that younger individuals have a more lumen-rich choroid for their choroidal thickness than older individuals. *Ophthalmology Science 2021;1:100033* © *2021 by the American Academy of Ophthalmology. This is an open access article under the CC BY-NC-ND license (http://creativecommons.org/licenses/by-nc-nd/4.0/).*

Supplemental material available at www.ophthalmologyscience.org.

The choroid, a posterior part of the uvea, is a membranous tissue lying between the retina and sclera. It comprises abundant vessels and stromal tissue and is rich in melanocytes. Because of these anatomic and histologic characteristics, the choroid is multifunctional and involved in the nourishment of the outer retina, regulation of the temperature of the retina, regulation of intraocular pressure (IOP), and absorption of excess light.[1] Thus, impairment of the choroid can cause numerous ocular diseases, including age-related macular degeneration (AMD), central serous chorioretinopathy (CSC), and high-myopia−related chorioretinal atrophy.[2–4] Additionally, recent advancements in OCT technology have facilitated detailed noninvasive investigations of the choroidal structure, leading to the definition of the new disease concept, pachychoroid.[5,6] The term *pachychoroid* indicates a thick choroid ("pachy-" [prefix]: thick).

https://doi.org/10.1016/j.xops.2021.100033
ISSN 2666-9145/21

In this context, the clinical significance of parameters for the choroid, particularly choroidal thickness, is increasing. Nevertheless, despite the importance of the criterion for the normal thickness of the choroid, a uniform cutoff thickness value may be difficult to identify because the thickness can be influenced by a variety of factors, including age, axial length (AL), refractive error, and blood pressure.[7–13] Thus, as we discussed in a previous report,[14] these parameters should be considered together to understand the relationship between choroidal thickness and its pathogenesis. Furthermore, several methods have been proposed to quantify the variation of histologic choroidal structure, such as choroidal vascularity index (CVI) and choroidal intensity, which allow for understanding the choroid in more detail. To apply our wider understanding of the choroid to clinical practice, it is essential to accumulate epidemiologic data for the choroidal condition in healthy populations; however, the epidemiologic features of the choroidal condition have been investigated in only a few cohorts.[7–9]

In this article, we report fundamental epidemiologic data for the choroidal condition using a large general Japanese cohort, the Nagahama Prospective Cohort for Comprehensive Human Bioscience (the Nagahama Study; n = 9850). Although the choroidal thickness of normal adult individuals has been reported in multiple studies,[7–13,15–25] all these studies included a small number of individuals (n < 1000), except for the Beijing Eye Study (n = 3233) and Singapore Epidemiology of Eye Diseases Study (SEEDS; n = 1619). To the best of our knowledge, the current study provides the largest normative data of choroidal thickness to date. In addition, we also present the distribution of choroidal intensity and CVI, which are recently introduced indicators of the choroidal brightness in OCT and are thought to correlate negatively and positively, respectively, with the dilation of choroidal vessels.[25–28]

Methods

This retrospective cross-sectional study followed the tenets of the Declaration of Helsinki. This study was also approved by the ethics committee of the Kyoto University Graduate School of Medicine and the Nagahama Municipal Review Board. Written informed consent was obtained from all participants.

Study Participants and Data Collection

We analyzed data from the second visit of the Nagahama Study obtained between 2013 and 2016. Although a detailed description of the Nagahama Study is provided elsewhere,[29,30] we summarized it briefly in the Supplemental Note (available https://www.ophthalmologyscience.org/). The present study analyzed a total of 9850 individuals 35 to 80 years of age.

All participants underwent a standardized ophthalmic examination, physical examinations, and blood tests. The standardized ophthalmic examination included measurement of the spherical equivalent (SE; ARK-530A; Nidek), IOP measurement by noncontact tonometry (full autotonometer TX-20P; Canon), central corneal thickness measurement (full autotonometer TX-20P), AL measurements by partial coherence interferometry (IOL Master; Carl Zeiss Meditec, Inc), color fundus photography (CR- DG10; Canon), and spectral-domain OCT (RS-3000 Advance; Nidek). Intraocular pressure and central corneal thickness were measured only from July 2013 through February 2016. Using OCT, a macular cross-scan of the right eye was performed in both normal and enhanced-depth modes. The scan width was 6 mm before February 2015 and 9 mm thereafter.

The following participants were excluded from this analysis: those without data for the right eye (n = 38), those for whom enhanced depth imaging (EDI) OCT images could not be obtained or the image quality was too poor to detect visually the entire layer of the choroid just under the fovea (n = 372), and those who had macular-involving disease (n = 115).

A questionnaire was administered to ascertain the history of cataract surgery, other ocular surgeries, and ocular laser treatment (including photocoagulation). The presence or absence of contact lens wear on the inspection day was recorded. Individuals who had undergone ocular surgery (excluding cataract surgery), ocular laser treatment, or both were excluded from all analyses. Additionally, individuals who had undergone cataract surgery were excluded from analyses of SE. Individuals who were unable to remove their contact lenses for special reasons also were excluded from analyses of SE, IOP, and central corneal thickness.

Measurement and Calculation of Choroidal Parameters

The inner limiting membrane, outer border of the nerve fiber layer (NFL), and Bruch's membrane in each EDI OCT image were detected automatically by the built-in software. Using the same software, the segmentation of the Bruch's membrane was corrected manually, and the outer border of the choroid was segmented manually as wide as visually detectable because the software was not equipped with an automated choroidal segmentation algorithm (Fig 1B). These manual procedures were performed by a retina specialist (Y.H.) and double-checked by a senior retina specialist (M.M.). In case of disagreement, the segmentation was corrected partially after discussion to determine the final grade. The choroidal thickness, defined as the distance between the Bruch's membrane and the outer border of the choroid, was measured at all points in the area where the outer border of the choroid was segmented. The subfoveal choroidal thickness (SFCT) was defined as the thickness just under the fovea. The parafoveal choroidal thickness (PFCT) was defined as the thickness in a 6-mm-wide area centered at the fovea and analyzed only for participants with available choroidal thickness in the entirety of that area. For the analysis of SFCT, the mean values of horizontal and vertical scans were used. For the analysis of PFCT, the mean values calculated for each of the following 6 areas were used: 2-mm-wide areas centered at the fovea in horizontal and vertical scan, and those centered at the points 2 mm away from the fovea in the nasal, temporal, superior, and inferior directions.

For participants who underwent a 9-mm scan, we calculated the normalized choroidal intensity (NCI) for a 6-mm width around the fovea, which provided an estimate of the absolute brightness of the choroid in OCT and was thought to reflect the dilation of choroidal vessels. The concept of normalization involves correction of choroidal intensity using the brightness of the vitreous body and NFL as reference values for low and high brightness, respectively, to minimize the effects of several factors, such as media opacity and scan tilt, and to enable comparison of the choroidal intensity between individuals. We performed this procedure with EDI OCT, and the calculated value was referred to as NCI obtained with EDI (NCI_{EDI}). Although the detailed calculation method has been described elsewhere,[27] we briefly summarize it here. First, we calculated the mean values of the vitreous intensity, NFL intensity, and unnormalized choroidal intensity from the scan pixel measurements by ImageJ software (National Institutes of Health). Then, NCI_{EDI} was calculated as follows:

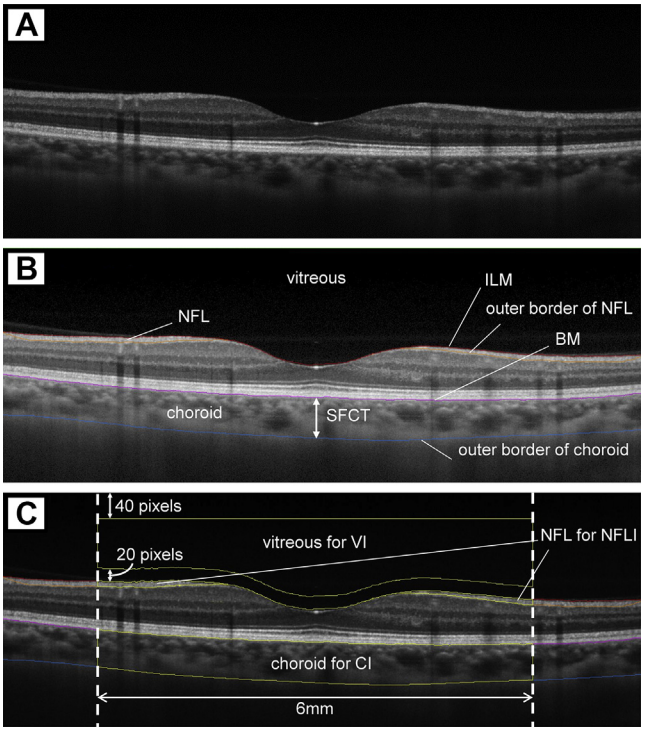

Figure 1. Measurement of subfoveal choroidal thickness (SFCT) and normalized choroidal intensity obtained with enhanced depth imaging (NCI_{EDI}). **A**, Raw unsegmented OCT image with enhanced depth imaging. **B**, Enhanced depth imaging OCT image after automatic and manual segmentation. The vitreous body was detected as the area over the inner limiting membrane (ILM). The nerve fiber layer (NFL) was detected as the area between the ILM and the outer border of the NFL. The choroid was detected as the area between the Bruch's membrane (BM) and the outer border of the choroid. The SFCT was defined as the distance between the BM and the outer border of the choroid under the fovea. **C**, Pixels in a range of 6 mm around the fovea were used for measurement of mean vitreous intensity (VI), nerve fiber layer intensity (NFLI), and choroidal intensity (CI). In particular, for measurement of VI, the vitreous area, excluding the upper 40 and lower 20 pixels, was used. Normalized choroidal intensity obtained with enhanced depth imaging was calculated as follows: NCI_{EDI} = (mean CI − mean VI) / mean NFLI.

NCI_{EDI} = (mean choroidal intensity − mean vitreous intensity) / mean NFL intensity. The resultant NCI_{EDI} is unitless. In this procedure, to define the respective layers, the boundaries decided automatically and manually by built-in software were used, as described above. Especially for measuring vitreous intensity, the vitreous area excluding the upper 40 pixels (the upper edge of the image that can contain a lot of noise) and the lower 20 pixels (the vitreoretinal border region where the brightness can increase because of the posterior vitreous membrane) was used. The measurement procedure and calculation of NCI_{EDI} are demonstrated in Figure 1. For the analysis of NCI_{EDI}, the mean values of horizontal and vertical scans were used.

For all participants, CVI was calculated and analyzed. Although the detailed calculation method has been described elsewhere,[28] we summarize it here briefly. First, the entire image of the horizontal B-scan was binarized using the Niblack method. Second, a region of the choroid 1.5-mm wide centered at the fovea center was extracted. Third, in the extracted area, the total choroidal area and the dark area (luminal area) were measured. The CVI was computed as the percentage of luminal area to total choroidal area.

Table 1. Participants' Demographic Characteristics and Standardized Values of Choroidal Parameters

Characteristics	Data
Sex (male/female)	2839 (32.0)/6042 (68.0)
Age (yrs)	57.6 ± 12.4
Body mass index (kg/m^2)	22.2 ± 3.3
Central systolic blood pressure (mmHg)	130.1 ± 19.4
HbA1c (%)	5.55 ± 0.49
High-density lipoprotein (mg/dL)	67.8 ± 17.4
Low-density lipoprotein (mg/dL)	118.4 ± 29.2
Intraocular pressure (mmHg)	14.6 ± 3.0
Central corneal thickness (μm)	543.88 ± 28.70
Axial length (mm)	24.11 ± 1.38
Spherical equivalent (D)	−1.47 ± 2.89
Subfoveal choroidal thickness (μm)*	291.2
NCI_{EDI} (unitless)*,†	0.653
Choroidal vascularity index (%)*	66.88

D = diopter; HbA1c = glycated hemoglobin; NCI_{EDI} = normalized choroidal intensity obtained with enhanced depth imaging.
Data are presented as mean±standard deviation, mean, or no. (%), unless otherwise indicated.
*Age-sex standardized values are shown.
†Number of eligible participants was 4561.

Similar to the NCI_{EDI} measurements, we used the boundaries determined automatically and corrected manually by the built-in software to define the respective layers. The measurement procedure and calculation of CVI were performed using Fiji open source software.[31]

Basic Clinical Parameters

Basic clinical parameters, including physical examination findings and plasma marker concentrations, were obtained from all participants. Age was calculated by dividing the number of days from birth to the date of examination by 365. Body mass index was calculated as follows: body mass index = weight / (height)^2 (kg/m^2). We measured central systolic blood pressure by using commercially available equipment (HEM-9000AI; Omron Healthcare), as reported previously.[32,33] Briefly, the participants' radial arterial waveform and brachial blood pressure after resting in the sitting position for 5 minutes were measured simultaneously. The measurements were measured twice, and the mean value was used for the analysis. The absolute pressure of the late systolic peak of the radial arterial waveform was defined as the central systolic blood pressure.

Statistical Analysis

Continuous data are shown as mean and standard deviation or standard error. Categorical data are shown as count and proportion. Because the age and sex distribution of the cohort deviated from those of the Japanese population, we calculated the age-sex standardized mean values of SFCT, NCI_{EDI}, and CVI. We standardized the current data to the population statistics published by the Japanese government[34] and calculated the population estimates of SFCT, NCI_{EDI}, and CVI stratified by age and sex. We also analyzed the distribution of NCI_{EDI} stratified by age and SFCT. The unpaired *t* test was performed to examine the differences in SFCT and NCI_{EDI} between sexes in each age category. The distribution of PFCT was stratified by age, sex, and area and was analyzed in each scan direction. A paired *t* test with Bonferroni correction was performed to examine the difference in PFCT

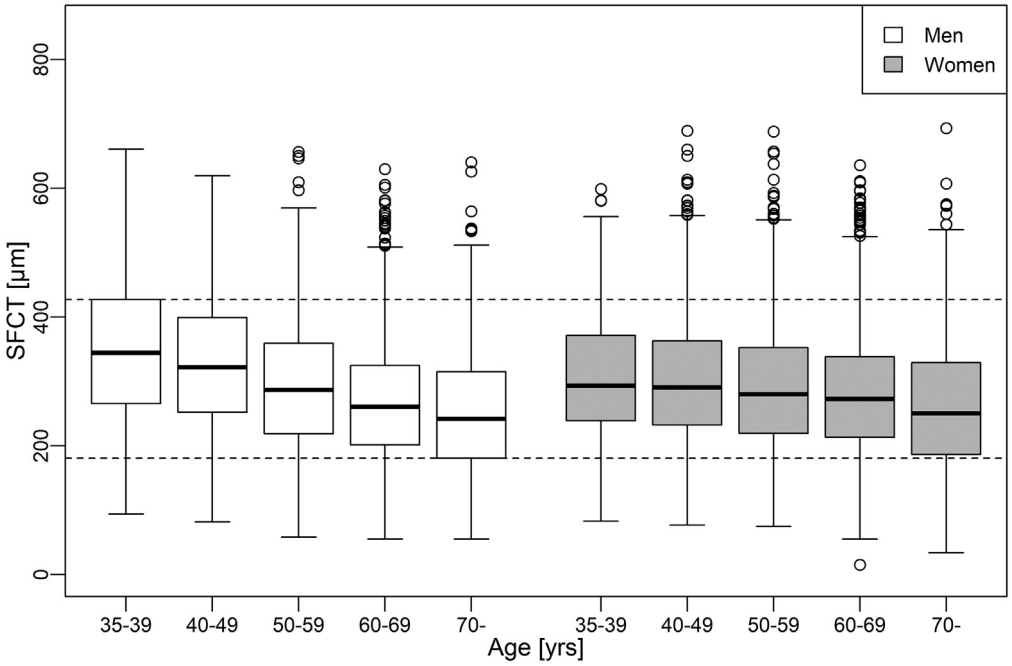

Figure 2. Boxplot showing the distribution of subfoveal choroidal thickness (SFCT) stratified by age and sex. The smallest first quartile (181.0 μm in men ≥ 70 years of age) and the largest third quartile (427.1 μm in men < 40 years of age) are shown as dotted lines for reference. In both men and women, SFCT was associated negatively with age ($P < 0.001$). Note that men showed a significantly thicker choroid than women among younger participants younger than 50 years ($P < 0.001$), and no statistically significant difference in choroidal thickness was found between sexes among older participants 50 years of age or older. This suggested the interaction between age and sex on SFCT.

between the areas in each sex and age category. The Jonckheere-Terpstra test was performed to examine the trends in these stratified data.

To evaluate the contributions of age, sex, AL, and SE to SFCT, we conducted linear regression analysis with adjustments for known possible contributing factors. In addition, to evaluate the associations of age, sex, AL, and SE with NCI_{EDI} and CVI, we also conducted linear regression analysis adjusted for known contributing factors, including choroidal thickness. Normalized choroidal intensity obtained with EDI was used after $\log_{10}$-transformation.

P values less than 0.05 were considered to be statistically significant. The statistical analyses were performed using R software version 4.1.0 (R Foundation for Statistical Computing).

Results

Finally, 8881 participants were included in the current study. Participants' clinical characteristics are shown in Table 1. The number of women was approximately twice as large as the number of men. The mean age was 57.6 ± 12.4 years. The mean IOP, AL, and SE were 14.6 ± 3.0 mmHg, 24.11 ± 1.38 mm, and −1.47 ± 2.89 diopters, respectively. The age-sex standardized SFCT, NCI_{EDI}, and CVI were 291.2 μm, 0.653, and 66.88%, respectively.

The age-sex stratified distribution of SFCT is shown in Figure 2, and the age-sex stratified population estimates of SFCT, NCI_{EDI}, and CVI are shown in Table 2. Although mean SFCT did not differ significantly between men and women overall ($P = 0.87$), men showed a significantly thicker choroid than women among the younger participants (35−40 years of age: 346.9 ± 6.8 μm vs. 307.2 ± 3.8 μm [$P < 0.001$]; 40−50 years: 329.1 ± 4.4 μm vs. 302.3 ± 2.6 μm [$P < 0.001$]). In both men and women, SFCT was associated negatively with age ($P < 0.001$). Similarly, although mean NCI_{EDI} did not significantly differ between men and women overall ($P = 0.21$), men tended to show lower intensity than women among the younger participants (35−40 years of age: 0.533 ± 0.021 vs. 0.572 ± 0.012 [$P = 0.11$]; 40−50 years of age: 0.548 ± 0.010 vs. 0.596 ± 0.007 [$P < 0.001$]). In both men and women, NCI_{EDI} was associated positively with age ($P < 0.001$). Choroidal vascularity index was significantly higher in men than in women overall (66.97 ± 0.06% vs. 66.79 ± 0.04%; $P = 0.015$) and men tended to show significantly higher CVI than women among the younger participants (35−40 years of age: 67.65 ± 0.14% vs. 67.12 ± 0.11% [$P = 0.004$]; 40−50 years of age: 67.42 ± 0.10 vs. 66.86 ± 0.08 [$P < 0.001$]). Overall, CVI was associated negatively with age ($P < 0.001$).

The results of linear regression for SFCT are shown in Table 3. As expected, age, sex, the interaction term of age and sex, AL, and SE were associated significantly with SFCT ($P < 0.001$). This model showed that SFCT decreased by 28.15 μm for a 1-mm elongation of AL and by 6.23 μm for a 1-diopter myopic shift. Considering the interaction term of age and sex, SFCT decreased by 4.05 μm for each year of age in men and 2.79 μm for each year of age in women.

Parafoveal choroidal thickness was analyzed in 7280 participants. The age- and sex-stratified PFCT distribution is shown in Figure 3. In the horizontal scan (Fig 3A), PFCT was thickest in the foveal area, followed by the temporal area and nasal area (289.7 ± 1.2 μm vs. 280.4 ± 1.0 μm vs. 222.8 ± 1.1

Table 2. Age-Sex Stratified Population Estimates of Choroidal Parameters

Parameter	Age (yrs)	Men		Women		All		P Value*
		Mean (Standard Error)	*No. (%)*	*Mean (Standard Error)*	*No. (%)*	*Mean (Standard Error)*	*No. (%)*	
SFCT (μm)	35–39	346.9 (6.8)	244 (2.7)	307.2 (3.8)	637 (7.2)	318.2 (3.4)	881 (9.9)	< 0.001
	40–49	329.1 (4.4)	555 (6.2)	302.3 (2.6)	1372 (15.4)	310.0 (2.3)	1927 (21.7)	< 0.001
	50–59	297.9 (5.0)	436 (4.9)	292.9 (2.8)	1335 (15.0)	294.1 (2.4)	1771 (19.9)	0.37
	60–69	271.5 (3.4)	860 (9.7)	279.6 (2.3)	1753 (19.7)	277.0 (1.9)	2613 (29.4)	0.049
	70+	252.5 (3.5)	744 (8.4)	262.5 (3.4)	945 (10.6)	258.1 (2.5)	1689 (19.0)	0.042
	All	288.3 (2.0)	2839 (32.0)	287.9 (1.3)	6042 (68.0)	288.1 (1.1)	8881 (100.0)	0.87
P value†		< 0.001		< 0.001		<0 .001		
NCI_{EDI} (unitless)	35–39	0.533 (0.021)	86 (1.9)	0.572 (0.012)	212 (4.6)	0.560 (0.011)	298 (6.5)	0.11
	40–49	0.548 (0.010)	302 (6.6)	0.596 (0.007)	717 (15.7)	0.582 (0.006)	1019 (22.3)	< 0.001
	50–59	0.620 (0.012)	285 (6.2)	0.628 (0.007)	812 (17.8)	0.626 (0.006)	1097 (24.1)	0.55
	60–69	0.685 (0.011)	455 (10.0)	0.676 (0.008)	900 (19.7)	0.679 (0.007)	1355 (29.7)	0.53
	70+	0.796 (0.016)	364 (8.0)	0.791 (0.015)	428 (9.4)	0.794 (0.011)	792 (17.4)	0.81
	All	0.663 (0.007)	1492 (32.7)	0.653 (0.004)	3069 (67.3)	0.657 (0.004)	4561 (100.0)	0.21
P value†		< 0.001		< 0.001		< 0.001		
CVI (%)	35–39	67.65 (0.14)	244 (2.7)	67.12 (0.11)	637 (7.2)	67.27 (0.09)	881 (9.9)	0.004
	40–49	67.42 (0.10)	555 (6.2)	66.86 (0.08)	1372 (15.4)	67.03 (0.06)	1927 (21.7)	< 0.001
	50–59	66.85 (0.15)	436 (4.9)	66.82 (0.08)	1335 (15.0)	66.82 (0.07)	1771 (19.9)	0.84
	60–69	66.93 (0.11)	860 (9.7)	66.81 (0.09)	1753 (19.7)	66.85 (0.07)	2613 (29.4)	0.39
	70+	66.52 (0.15)	744 (8.4)	66.38 (0.14)	945 (10.6)	66.44 (0.10)	1689 (19.0)	0.47
	All	66.97 (0.06)	2839 (32.0)	66.79 (0.04)	6042 (68.0)	66.85 (0.04)	8881 (100.0)	0.015
P value†		< 0.001		0.39		< 0.001		

CVI = choroidal vascularity index; NCI_{EDI} = normalized choroidal intensity obtained with enhanced depth imaging; SFCT = subfoveal choroidal thickness.
*Difference between sexes was tested by unpaired *t* test.
†Association with age strata was tested by Jonckheere-Terpstra test.

μm; $P < 0.001$). In the vertical scan (Fig 3B), PFCT showed no significant difference between the superior area and the foveal area (297.2 ± 1.1 μm vs. 296.3 ± 1.2 μm; $P = 0.06$), whereas PFCT was thinnest in the inferior area (276.9 ± 1.1 μm; $P < 0.001$). The population estimates of PFCT stratified by age, sex, and area are shown in Supplemental Table 1 (available at https://www.ophthalmologyscience.org/). In all areas, PFCT was significantly thicker in men than women among younger participants (35–50 years of age; $P < 0.001$), showed no significant difference between sexes in middle-aged participants (50–65 years of age; $P > 0.05$), and tended to be thinner in men than women in older participants (older than 65 years; $P = 0.040$ in the inferior area, $P = 0.004$ in the nasal area, and $P < 0.001$ in the other areas).

Normalized choroidal intensity obtained with EDI was analyzed in 4561 participants. The distribution of NCI_{EDI} stratified by age and SFCT is shown in Figure 4. In all age strata, NCI_{EDI} was correlated negatively with SFCT ($P < 0.001$), that is, NCI_{EDI} decreased as the choroid became thicker. In each SFCT category (except for < 100 μm), NCI_{EDI} tended to increase with age (SFCT between 100 and 500 μm, $P < 0.001$; SFCT > 500 μm, $P = 0.064$). In the scatterplots shown in Supplemental Figures 1 and 2 (available at https://www.ophthalmologyscience.org/), the negative and positive correlation between NCI_{EDI} or CVI and SFCT increased in strength as the patients became older. Table 4 summarizes the results of the linear regression analysis for NCI_{EDI} and CVI. On the basis of Supplemental Figures 1 and 2, we included an interaction

Table 3. Multivariable Analysis of Associations with Subfoveal Choroidal Thickness

Parameters	β	95% Confidence Interval for β	Standardized β	P Value
Age	−4.05	−4.35 to −3.75	−0.403	< 0.001
Sex (female)	−20.16	−25.06 to −15.27	−0.093	< 0.001
Interaction term of age and sex (female)	1.26	0.91–1.60	0.074	< 0.001
Axial length	−28.15	−30.86 to −25.44	−0.375	< 0.001
Spherical equivalent	6.23	4.94–7.52	0.176	< 0.001
Intraocular pressure	−0.89	−1.65 to −0.12	−0.026	0.023
Body mass index	0.59	−0.12 to 1.29	0.019	0.10
Low-density lipoprotein	0.06	−0.02 to 0.13	0.016	0.13
High-density lipoprotein	0.07	−0.06 to 0.21	0.013	0.27
Central corneal thickness	0.03	−0.04 to 0.11	0.010	0.37
Central systolic blood pressure	0.03	−0.09 to 0.15	0.005	0.66
Glycated hemoglobin	−0.33	−4.74 to 4.09	−0.002	0.88

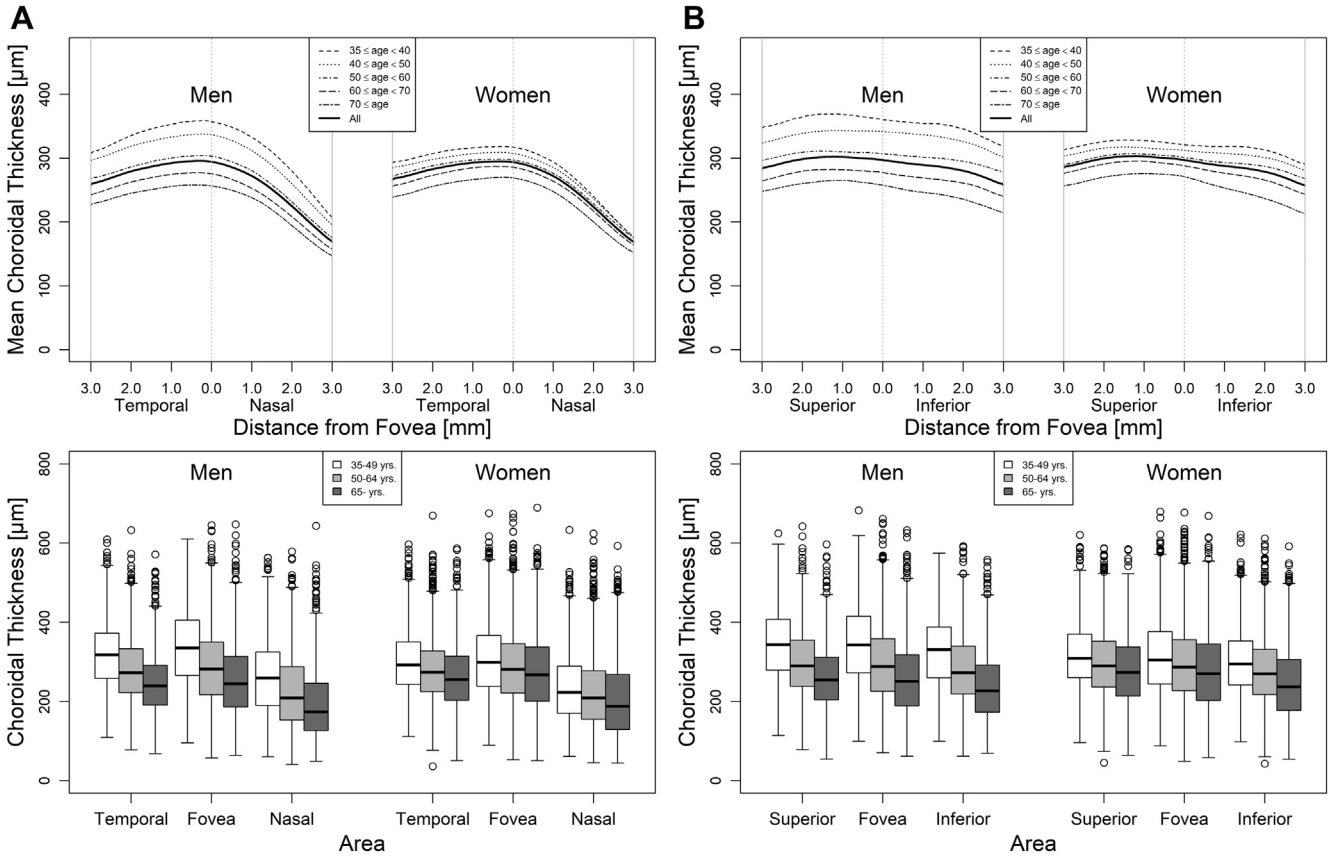

Figure 3. Age-sex stratified parafoveal choroidal thickness (PFCT). **A**, **B**, Line graphs and boxplots showing the choroidal thickness according to the distance from the fovea, stratified by age and sex: results from the (**A**) horizontal scan and (**B**) vertical scan. **A**, For any stratum, PFCT was thickest in the foveal area, followed by the temporal area and the nasal area. **B**, For any stratum, PFCT showed no significant difference between the superior area and the foveal area, whereas it was thinnest in the inferior area ($P < 0.001$). **A**, **B**, Regardless of sex and area, PFCT was associated negatively with age ($P < 0.001$). Note that men showed a greater decrease in PFCT with age than women in all areas.

term for age and SFCT. Although AL and SE were not associated significantly with NCI_{EDI} ($P = 0.069$ and $P = 0.63$, respectively), NCI_{EDI} was associated significantly with age, SFCT, and their interaction term, as expected ($\beta = 1.90 \times 10^{-3}$, standardized $\beta = 0.161$ [$P < 0.001$]; $\beta = -1.09 \times 10^{-3}$, standardized $\beta = -0.749$ [$P < 0.001$]; and $\beta = -0.01 \times 10^{-3}$, standardized $\beta = -0.062$ [$P < 0.001$]; respectively). Similar to NCI_{EDI}, CVI was associated significantly with age, SFCT, and their interaction term ($\beta = -1.74 \times 10^{-4}$, standardized $\beta = 0.091$ [$P < 0.001$]; $\beta = 0.60 \times 10^{-4}$, standardized $\beta = 0.259$ [$P < 0.001$]; and $\beta = 0.02 \times 10^{-4}$, standardized $\beta = 0.130$ [$P < 0.001$]; respectively) and also associated with sex, AL, and SE ($\beta = -26.20 \times 10^{-4}$, standardized $\beta = -0.051$ [$P < 0.001$]; $\beta = -15.41 \times 10^{-4}$, standardized $\beta = -0.089$ [$P < 0.001$]; and $\beta = 9.31 \times 10^{-4}$, standardized $\beta = 0.113$ [$P < 0.001$]; respectively).

Discussion

With the development of the EDI technique for OCT,[35] the choroid increasingly is being recognized as a clinically important structure, because the pathologic features of the choroid have been revealed to be associated with various ocular diseases such as AMD, high myopia, Vogt-Koyanagi-Harada disease, and CSC.[36] In particular, the concept of pachychoroid disease has gained attention because pachychoroid pathologic features, such as a thickened choroid and dilated choroidal vessels, can cause retinal pigment epithelium damage and choroidal neovascularization, sometimes resulting in irreversible visual loss. These conditions are termed pachychoroid pigment epitheliopathy and pachychoroid neovasculopathy, respectively, and together with CSC, they constitute the core elements of pachychoroid-related diseases.[37,38]

In previous studies,[39,40] we investigated the molecular biological mechanisms underlying pachychoroid through genome-wide association studies of choroidal thickness and CSC. We found that *CFH* and *VIPR2* were the important genetic determinants of choroidal thickness[39] and that these genes together with *TNFRSF10A* and *GATA5* are the susceptibility genes for CSC.[40] We also reported the clinical importance of defining *pachychoroid* for differentiating pachychoroid neovasculopathy from AMD, because pachychoroid neovasculopathy often seems to be AMD and is misdiagnosed as a result, especially in Asia, where

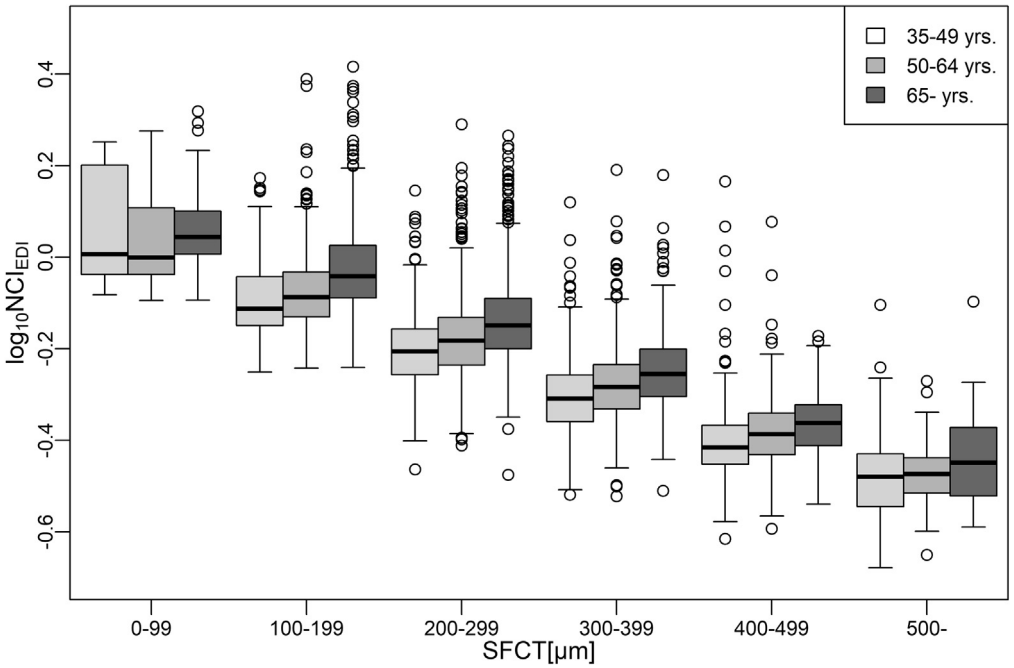

Figure 4. Boxplot of the distribution of $\log_{10}$-transformed normalized choroidal intensity obtained with enhanced depth imaging (NCI_{EDI}) stratified by age and subfoveal choroidal thickness (SFCT). In all age categories, NCI_{EDI} was correlated negatively with SFCT ($P < 0.001$). In each SFCT category (except for < 100 μm), NCI_{EDI} tended to increase with age (SFCT 100–500 μm, $P < 0.001$; SFCT > 500 μm, $P = 0.064$).

pachychoroid diseases are common.[14,41] Subsequent studies also support this idea, and the criteria for a thick choroid currently are the subject of debate.[37,42,43] However, despite the increasing clinical importance of the choroid, only a few large-scale cohort studies have provided normative data for choroidal thickness.[7,8] In this study, we reported the age-sex stratified normative data for choroidal parameters, that is, choroidal thickness and choroidal intensity, using a relatively large general Japanese cohort from the Nagahama Study (n = 9850).

The age-sex standardized SFCT (291.2 μm) in the present study was thicker than that reported in earlier

Table 4. Multivariable Analysis of Associations with Normalized Choroidal Intensity Obtained with Enhanced Depth Imaging and Choroidal Vascularity Index

	Normalized Choroidal Intensity Obtained with Enhanced Depth Imaging				Choroidal Vascularity Index			
Parameters	β ($\times 10^{-3}$)	95% Confidence Interval for β ($\times 10^{-3}$)	Standardized β	P Value	β ($\times 10^{-4}$)	95% Confidence Interval for β ($\times 10^{-4}$)	Standardized β	P Value
Age	1.90	1.54–2.26	0.161	< 0.001	−1.74	−2.23 to −1.25	−0.091	< 0.001
Sex (female)	7.12	−0.62 to 14.85	0.023	0.072	−26.20	−37.23 to −15.17	−0.051	< 0.001
Axial length	−4.15	−8.61 to 0.32	−0.038	0.069	−15.41	−21.67 to −9.15	−0.089	< 0.001
Spherical equivalent	−0.51	−2.58 to 1.56	−0.010	0.63	9.31	6.39–12.23	0.113	< 0.001
SFCT	−1.09	−1.13 to −1.05	−0.749	<0.001	0.60	0.55–0.66	0.259	< 0.001
Interaction term of age and SFCT	−0.01	−0.01 to 0.00	−0.062	< 0.001	0.02	0.02–0.03	0.130	< 0.001
Low-density lipoprotein	−0.08	−0.19 to 0.03	−0.016	0.15	0.09	−0.07 to 0.25	0.011	0.28
High-density lipoprotein	−0.13	−0.34 to 0.08	−0.016	0.22	−0.01	−0.31 to 0.28	−0.001	0.93
Body mass index	0.58	−0.53 to 1.69	0.013	0.31	0.81	−0.76 to 2.38	0.011	0.31
Interocular pressure	0.51	−0.69 to 1.72	0.010	0.41	0.24	−1.47 to 1.95	0.003	0.78
Glycated hemoglobin	2.86	−4.07 to 9.80	0.010	0.42	−10.63	−20.52 to −0.74	−0.022	0.035
Central corneal thickness	−0.04	−0.16 to 0.08	−0.007	0.54	−0.03	−0.20 to 0.14	−0.004	0.71
Central Systolic blood pressure	−0.02	−0.22 to 0.17	−0.003	0.80	−0.05	−0.32 to 0.23	−0.004	0.73

SFCT = subfoveal choroidal thickness.
The data for normalized choroidal intensity obtained with enhanced depth imaging and choroidal vascularity index were $\log_{10}$-transformed before analysis.

population-based cohort studies: 253.8 ± 107.4 μm in the Beijing Eye Study, which investigated 3233 eyes of 3233 Chinese individuals 50 to 93 years of age (mean, 64.3 ± 9.6 years),[7] and 255.2 ± 102.6 μm in the SEEDS, which investigated 2794 eyes of 1619 Chinese, Indian, and Malay individuals 50 to 90 years of age (mean, 60.9 ± 7.7 years).[8] This difference may be attributed to the fact that the current study included younger individuals, who tend to have a thicker choroid, than the previous studies. The effect sizes in the Beijing Eye Study and SEEDS were −44.7 μm and −32.1 μm per 1-mm axial elongation, respectively, and −4.12 μm and −4.33 μm per 1 year of age, respectively, which are almost compatible with the data obtained in the current study (Table 3). Parafoveal choroidal thickness also showed a tendency compatible with the result of SEEDS,[8] which analyzed macular volume scans; PFCT was thickest in the superior area, followed by the foveal area, the temporal area, the inferior area, and the nasal area. However, the significant interaction between age and sex on SFCT is a novel finding of the current study (Fig 2; Tables 2 and 3).

The significant interaction between age and sex on SFCT ($P < 0.001$) indicates that the effect of age on SFCT differs significantly between sexes. In fact, Figure 2 and Table 2 show that men harbor a significantly thicker choroid than women among participants younger than 50 years, whereas no statistically significant differences were found among older participants after Bonferroni correction, with men tending to show a thinner choroid. Because this significant interaction was noted even after adjusting for possible confounders, including refractive status and AL, and a similar trend also was observed in PFCT (Fig 3; Supplemental Table 1), we believe that the results are robust. The most important pachychoroid spectrum disease, CSC, is known to occur predominantly in men (male-to-female ratio, 7:1) in their 40s. The current distribution of choroidal thickness may suggest the presence of the underlying choroidal pathologic features of CSC among younger men. To date, although the choroidal thickness in men has been reported to be more than that in women,[7–9] age-sex stratified analysis has not been conducted, probably because of the limited sample sizes of previous reports. The novel finding of the current study should be replicated in other cohorts and large epidemiologic consortiums, such as the European Eye Epidemiology Consortium[44] and the Asian Eye Epidemiology Consortium.[45]

Pachychoroid is characterized not only by choroidal thickness, but also by dilation of choroidal vessels.[37,42] Several methods for quantifying choroidal vessel dilation have been proposed to improve our understanding of the choroidal structure in more detail. For example, Branchini et al introduced the light-to-dark ratio, which is an indicator of the ratio of the choroidal stromal area to the choroidal vessel lumen area.[21] Sonoda et al,[46] using the freely available ImageJ software, evaluated the proportion of black (luminal) and white (interstitial) areas on binarized EDI choroidal images, and this evaluation method was later modified into CVI by Agrawal et al.[25] Similarly, Balasubramanian et al calculated the NCI, which is the absolute brightness of the choroid with reference to the dark structure vitreous body and the bright structure NFL.[27] The age-sex standardized CVI (66.88%; n = 8881) in the present study was consistent with that reported in an earlier population-based study (mean ± standard deviation, 65.61 ± 2.33%; n = 345).[25]

These parameters, that is, indicators of choroidal vessel dilation, are known to correlate strongly with choroidal thickness,[25,27] which also has been observed in the current study (Fig 4; Supplemental Figs 1 and 2). In addition, our age-stratified analysis (Supplemental Figs 1 and 2) and multivariable analysis (Table 4) were the first to reveal that the strength of the correlation between SFCT and NCI_{EDI} or CVI varied with age ($P < 0.001$); younger individuals showed a more lumen-rich choroid for their choroidal thickness than older individuals. This is consistent with the findings of previous histologic reports in which blood vessels (low-intensity areas) decrease with age more predominantly than stromal tissue (high-intensity areas).[47–49] Although CVI was reported previously to be associated with only SFCT in a multivariable analysis,[25] we were able to find additional controlling factors because of a larger sample size, notably age, sex, AL, SE, and the interaction term of age and SFCT (Table 4). Age, SFCT, and their interaction term were associated significantly with both NCI_{EDI} and CVI, suggesting that these parameters represent similar aspects of the choroidal status, although not exactly the same. Further research is needed to clarify the clinical relevance and differences between these parameters. Considering choroidal thickness and brightness characterized different aspects of the choroidal structure, a combination of these parameters may allow differentiation of the pachychoroid spectrum.

The potential limitations of our study need to be mentioned. First, because the current study was a community-based one, the overall distributions of age and sex were different from those in the normal Japanese population. However, by using age-sex based stratification and standardization to present summary data, we believe we minimized its influence. Second, although the current study presented normative NCI_{EDI} data for the first time, these values need to be interpreted carefully. Because the current study used EDI OCT images, which increase the intensity of the choroid, unlike the findings in the original report proposing NCI, NCI_{EDI} is higher than NCI obtained with normal OCT images. However, because EDI is currently essential for evaluating the choroid, we believe that normative NCI_{EDI} data are rather important. Finally, the generalizability of these findings is limited to the Japanese population undergoing assessments with the SD-OCT RS-3000 Advance device. Further replication in other ethnicities and with various OCT methods is expected.

In summary, we present normative data for choroidal thickness, choroidal intensity, and CVI in Japanese individuals by using a large general Japanese population from the Nagahama Study. The current data indicated the

presence of a significantly thicker choroid in younger men, which might have some relationship to pachychoroid pathogenesis. The association analysis of SFCT with NCI_{EDI} and CVI suggested that younger individuals showed a more lumen-rich choroid for their choroidal thickness than older individuals. Further replication of these findings in larger cohorts such as an epidemiologic consortium is expected.

Footnotes and Disclosures

Originally received: March 16, 2021.
Final revision: May 31, 2021.
Accepted: June 2, 2021.
Available online: June 10, 2021. Manuscript no. D-21-00018.

[1] Department of Ophthalmology, Kyoto University Graduate School of Medicine, Kyoto, Japan.

[2] Center for Genomic Medicine, Kyoto University Graduate School of Medicine, Kyoto, Japan.

[3] Department of Ophthalmology, Osaka Red-Cross Hospital, Osaka, Japan.

[4] Center for Innovative Research and Education in Data Science, Institute for Liberal Arts and Sciences, Kyoto University, Kyoto, Japan.

[5] Graduate School of Public Health, Shizuoka Graduate University of Public Health, Shizuoka, Japan.

[6] Department of Ophthalmology, Otsu Red-Cross Hospital, Otsu, Japan.

*Members of the Nagahama Study Group: Takeo Nakayama, MD, PhD, Akihiro Sekine, PhD, Shinji Kosugi, MD, PhD, Yasuharu Tabara, PhD, and Fumihiko Matsuda, PhD.

Disclosure(s):
All authors have completed and submitted the ICMJE disclosures form.

The author(s) have made the following disclosure(s):

Y.M.: Lecturer — Santen Pharmaceutical Co, Ltd.

M.M.: Consultant and Lecturer — Santen Pharmaceuticals, Nevaker, Novartis Pharmaceuticals, Japan Alcon, HOYA, Kowa Pharmaceuticals, Senju Pharmaceuticals, Ellex, Johnson & Johnson, AMO Japan

H.T.: Financial support — Findex, Suntory; Nonfinancial support — Bayer Yakuhin, Novartis, Santen Pharmaceutical; Lecturer — Novartis

S.O.: Financial support — Alcon Japan, Bayer, Santen Pharma, Senju Pharma, Nidek, Novartis pharma

K.Y.: Lecturer — Novartis Pharma, Bayer Yakuhin, Santen Pharmaceutical, Alcon Pharmaceutical, Senju Pharmaceutical, Kowa Company, Canon, Chugai Pharmaceutical

A.T.: Advisory board — Santen Pharmaceutical, Senju Pharmaceutical, Alcon Japan, Alcon Pharma, Hoya, Bayer Yakuhin, Novartis Pharma, Chugai Pharmaceutical, Astellas, Eisai, Daiich-Sankyo, Janssen Pharmaceutical, Kyoto Drug Discovery & Development, Allergan Japan; Financial support — Canon, Findex, Santen Pharmaceutical, Kowa Pharmaceutical, Pfizer, AMO Japan, Senju Pharmaceutical, Wakamoto Pharmaceutical, Alcon Japan, Alcon Pharmaceutical, Otsuka Pharmaceutical, Tomey Corporation, Taiho Pharma, Hoya, Bayer Yakuhin, Novartis Pharmaceutical, Chugai Pharmaceutical, Astellas, Eisai, Daiich-Sankyo, Janssen Pharmaceutical, Kyoto Drug Discovery & Development, Allergan Japan, Sanwa Kagaku Kenkyusho, Nitten Pharmaceutical, Otsuka Pharmaceutical

Supported by the Ministry of Education, Culture, Sports, Science and Technology of Japan (grant nos.: 25293141, 26670313, 26293198, 17H04182, 17H04126, 17H04123, 18K18450, and 19K17634); Japan Society for the Promotion of Science (KAKENHI grant no: JP20H03841); Japan Agency for Medical Research and Development (Practical Research Project for Rare/Intractable Diseases grant nos.: ek0109070, ek0109283, ek0109196, and ek0109348; Comprehensive Research on Aging and Health Science Research Grants for Dementia R&D grant nos: dk0207006, dk0207027, and dk0110040; Program for an Integrated Database of Clinical and Genomic Information grant no.: kk0205008; Practical Research Project for Lifestyle-Related Diseases including Cardiovascular Diseases and Diabetes Mellitus grant nos: ek0210066, ek0210096, and ek0210116; and Research Program for Health Behavior Modification by Utilizing IoT grant nos: le0110005 and le0110013); the Takeda Medical Research Foundation; the Mitsubishi Foundation; the Daiwa Securities Health Foundation; and the Sumitomo Foundation.

HUMAN SUBJECTS: Human subjects were included in this study. The human ethics committees at the Kyoto University Graduate School of Medicine and the Nagahama Municipal Review Board approved the study. All research adhered to the tenets of the Declaration of Helsinki. All participants provided informed consent.

No animal subjects were included in this study.

Author Contributions:

Conception and design: Miyake, Tabara, Yamashiro

Analysis and interpretation: Mori, Miyake, Hosoda, Uji, Nakano, Takahashi, Muraoka, Miyata, Tamura, Ooto, Tabara, Yamashiro, Matsuda, Tsujikawa

Data collection: Mori, Miyake, Hosoda, Nakano, Matsuda

Obtained funding: Miyake, Tabara, Matsuda

Overall responsibility: Mori, Miyake, Hosoda, Uji, Nakano, Takahashi, Muraoka, Miyata, Tamura, Ooto, Tabara, Yamashiro, Matsuda, Tsujikawa

Abbreviations and Acronyms:
AL = axial length; **AMD** = age-related macular degeneration; **CSC** = central serous chorioretinopathy; **CVI** = choroidal vascularity index; **EDI** = enhanced depth imaging; **IOP** = intraocular pressure; **NCI** = normalized choroidal intensity; **NCI_{EDI}** = normalized choroidal intensity obtained with enhanced depth imaging; **NFL** = nerve fiber layer; **FCT** = parafoveal choroidal thickness; **SE** = spherical equivalent; **SEEDS** = Singapore Epidemiology of Eye Diseases Study; **SFCT** = subfoveal choroidal thickness; **OCT** = optical coherence tomography.

Keywords:
Choroidal epidemiology, Choroidal intensity, Nagahama Study, OCT, Subfoveal choroidal thickness.

Correspondence:
Masahiro Miyake, MD, PhD, MPH, Department of Ophthalmology and Visual Sciences, Kyoto University Graduate School of Medicine, 54 Shogoin-kawahara, Sakyo, Kyoto 606-8507, Japan. E-mail: miyakem@kuhp.kyoto-u.ac.jp.

References

1. Nickla DL, Wallman J. The multifunctional choroid. *Prog Retin Eye Res*. 2010;29(2):144–168.
2. Spaide RF, Hall L, Haas A, et al. Indocyanine green video-angiography of older patients with central serous chorioretinopathy. *Retina*. 1996;16(3):203–213.
3. Gomi F, Tano Y. Polypoidal choroidal vasculopathy and treatments. *Curr Opin Ophthalmol*. 2008;19(3):208–212.
4. Grossniklaus HE, Green WR. Choroidal neovascularization. *Am J Ophthalmol*. 2004;137(3):496–503.
5. Pang CE, Freund KB. *Pachychoroid neovasculopathy*. Retina. 2015;35(1):1–9.
6. Warrow DJ, Hoang QV, Freund KB. *Pachychoroid pigment epitheliopathy*. Retina. 2013;33(8):1659–1672.
7. Wei WB, Xu L, Jonas JB, et al. Subfoveal choroidal thickness: the Beijing Eye Study. *Ophthalmology*. 2013;120(1):175–180.
8. Song Y, Tham YC, Chong C, et al. Patterns and determinants of choroidal thickness in a multiethnic Asian population: the Singapore Epidemiology of Eye Diseases Study. *Ophthalmol Retina*. 2021;5(5):458–467.
9. Gupta P, Jing T, Marziliano P, et al. Distribution and determinants of choroidal thickness and volume using automated segmentation software in a population-based study. *Am J Ophthalmol*. 2015;159(2):293–301.e3.
10. Agawa T, Miura M, Ikuno Y, et al. Choroidal thickness measurement in healthy Japanese subjects by three-dimensional high-penetration optical coherence tomography. *Graefes Arch Clin Exp Ophthalmol*. 2011;249(10):1485–1492.
11. Michalewski J, Michalewska Z, Nawrocka Z, et al. Correlation of choroidal thickness and volume measurements with axial length and age using swept source optical coherence tomography and optical low-coherence reflectometry. *Biomed Res Int*. 2014;2014:639160.
12. Hirata M, Tsujikawa A, Matsumoto A, et al. Macular choroidal thickness and volume in normal subjects measured by swept-source optical coherence tomography. *Invest Ophthalmol Vis Sci*. 2011;52(8):4971–4978.
13. Li L, Yang ZK, Dong FT. [Choroidal thickness in normal subjects measured by enhanced depth imaging optical coherence tomography]. *Zhonghua Yan Ke Za Zhi*. 2012;48(9):819–823.
14. Miyake M, Ooto S, Yamashiro K, et al. Pachychoroid neovasculopathy and age-related macular degeneration. *Sci Rep*. 2015;5:16204.
15. Ikuno Y, Kawaguchi K, Nouchi T, Yasuno Y. Choroidal thickness in healthy Japanese subjects. *Invest Ophthalmol Vis Sci*. 2010;51(4):2173–2176.
16. Manjunath V, Taha M, Fujimoto JG, Duker JS. Choroidal thickness in normal eyes measured using Cirrus HD optical coherence tomography. *Am J Ophthalmol*. 2010;150(3):325–329.e1.
17. Shin JW, Shin YU, Cho HY, Lee BR. Measurement of choroidal thickness in normal eyes using 3D OCT-1000 spectral domain optical coherence tomography. *Korean J Ophthalmol*. 2012;26(4):255–259.
18. Margolis R, Spaide RF. A pilot study of enhanced depth imaging optical coherence tomography of the choroid in normal eyes. *Am J Ophthalmol*. 2009;147(5):811–815.
19. Rahman W, Chen FK, Yeoh J, et al. Repeatability of manual subfoveal choroidal thickness measurements in healthy subjects using the technique of enhanced depth imaging optical coherence tomography. *Invest Ophthalmol Vis Sci*. 2011;52(5):2267–2271.
20. Esmaeelpour M, Povazay B, Hermann B, et al. Three-dimensional 1060-nm OCT: choroidal thickness maps in normal subjects and improved posterior segment visualization in cataract patients. *Invest Ophthalmol Vis Sci*. 2010;51(10):5260–5266.
21. Branchini LA, Adhi M, Regatieri CV, et al. Analysis of choroidal morphologic features and vasculature in healthy eyes using spectral-domain optical coherence tomography. *Ophthalmology*. 2013;120(9):1901–1908.
22. Bhayana AA, Kumar V, Tayade A, et al. Choroidal thickness in normal Indian eyes using swept-source optical coherence tomography. *Indian J Ophthalmol*. 2019;67(2):252–255.
23. Lee SSY, Lingham G, Alonso-Caneiro D, et al. Choroidal thickness in young adults and its association with visual acuity. *Am J Ophthalmol*. 2020;214:40–51.
24. Moussa M, Sabry D, Soliman W. Macular choroidal thickness in normal Egyptians measured by swept source optical coherence tomography. *BMC Ophthalmol*. 2016;16:138.
25. Agrawal R, Gupta P, Tan KA, et al. Choroidal vascularity index as a measure of vascular status of the choroid: measurements in healthy eyes from a population-based study. *Sci Rep*. 2016;6:21090.
26. Velaga SB, Nittala MG, Vupparaboina KK, et al. Choroidal vascularity index and choroidal thickness in eyes with reticular pseudodrusen. *Retina*. 2020;40(4):612–617.
27. Balasubramanian S, Lei J, Nittala MG, et al. Association of drusen volume with choroidal parameters in nonneovascular age-related macular degeneration. *Retina*. 2017;37(10):1880–1887.
28. Agrawal R, Salman M, Tan KA, et al. Choroidal vascularity index (CVI)—a novel optical coherence tomography parameter for monitoring patients with panuveitis? *PLoS One*. 2016;11(1):e0146344.
29. Miyake M, Yamashiro K, Tabara Y, et al. Identification of myopia-associated WNT7B polymorphisms provides insights into the mechanism underlying the development of myopia. *Nat Commun*. 2015;6:6689.
30. Nakata I, Yamashiro K, Nakanishi H, et al. Prevalence and characteristics of age-related macular degeneration in the Japanese population: the Nagahama Study. *Am J Ophthalmol*. 2013;156(5):1002–1009.e2.
31. Schindelin J, Arganda-Carreras I, Frise E, et al. Fiji: an open-source platform for biological-image analysis. *Nat Methods*. 2012;9(7):676–682.
32. Hirata K, Kojima I, Momomura S. Noninvasive estimation of central blood pressure and the augmentation index in the seated position: a validation study of two commercially available methods. *J Hypertens*. 2013;31(3):508–515. discussion 515.
33. Kumagai K, Tabara Y, Yamashiro K, et al. Central blood pressure relates more strongly to retinal arteriolar narrowing than brachial blood pressure: the Nagahama Study. *J Hypertens*. 2015;33(2):323–329.
34. Statistics Bureau of Japan. Population by age (single years), sex and sex ratio—total population, Japanese population, October 1, 2018. e-Stat, Portal site of Official Statistics of Japan. Available at: https://www.e-stat.go.jp/en/stat-search/files?page=1&layout=datalist&toukei=00200524&tstat=000000090001&cycle=7&year=20180&month=0&tclass1=000

001011679&stat_infid=000031807138. Accessed May 10, 2020.
35. Wong IY, Koizumi H, Lai WW. Enhanced depth imaging optical coherence tomography. *Ophthalmic Surg Lasers Imaging*. 2011;42(4):S75−S84.
36. Mrejen S, Spaide RF. Optical coherence tomography: imaging of the choroid and beyond. *Surv Ophthalmol*. 2013;58(5):387−429.
37. Yanagi Y. Pachychoroid disease: a new perspective on exudative maculopathy. *Jpn J Ophthalmol*. 2020;64(4):323−337.
38. Yamashiro K, Hosoda Y, Miyake M, et al. Characteristics of pachychoroid diseases and age-related macular degeneration: multimodal imaging and genetic backgrounds. *J Clin Med*. 2020;9(7):2034.
39. Hosoda Y, Yoshikawa M, Miyake M, et al. CFH and VIPR2 as susceptibility loci in choroidal thickness and pachychoroid disease central serous chorioretinopathy. *Proc Natl Acad Sci U S A*. 2018;115(24):6261−6266.
40. Hosoda Y, Miyake M, Schellevis RL, et al. Genome-wide association analyses identify two susceptibility loci for pachychoroid disease central serous chorioretinopathy. *Commun Biol*. 2019;2:468.
41. Hosoda Y, Miyake M, Yamashiro K, et al. Deep phenotype unsupervised machine learning revealed the significance of pachychoroid features in etiology and visual prognosis of age-related macular degeneration. *Sci Rep*. 2020;10(1):18423.
42. Cheung CMG, Lee WK, Koizumi H, et al. Pachychoroid disease. *Eye (Lond)*. 2019;33(1):14−33.
43. Spaide RF. Disease expression in nonexudative age-related macular degeneration varies with choroidal thickness. *Retina*. 2018;38(4):708−716.
44. Delcourt C, Korobelnik JF, Buitendijk GH, et al. Ophthalmic epidemiology in Europe: the "European Eye Epidemiology" (E3) consortium. *Eur J Epidemiol*. 2016;31(2):197−210.
45. Rim TH, Kawasaki R, Tham YC, et al. Prevalence and pattern of geographic atrophy in Asia: the Asian Eye Epidemiology Consortium. *Ophthalmology*. 2020;127(10):1371−1381.
46. Sonoda S, Sakamoto T, Yamashita T, et al. Choroidal structure in normal eyes and after photodynamic therapy determined by binarization of optical coherence tomographic images. *Invest Ophthalmol Vis Sci*. 2014;55(6):3893−3899.
47. Ramrattan RS, van der Schaft TL, Mooy CM, et al. Morphometric analysis of Bruch's membrane, the choriocapillaris, and the choroid in aging. *Invest Ophthalmol Vis Sci*. 1994;35(6):2857−2864.
48. Lee WK, Baek J, Dansingani KK, et al. Choroidal morphology in eyes with polypoidal choroidal vasculopathy and normal or subnormal subfoveal choroidal thickness. *Retina*. 2016;36(Suppl 1):S73−S82.
49. Lee SY, Stetson PF, Ruiz-Garcia H, et al. Automated characterization of pigment epithelial detachment by optical coherence tomography. *Invest Ophthalmol Vis Sci*. 2012;53(1):164−170.